5th Fatigue Design Conference, Fatigue Design 2013

Characterization of fatigue damage in 304L steel by an acoustic emission method

A. OULD AMER[a] *, A-L. GLOANEC[a], S. COURTIN[b], C. TOUZE[a]

[a] ENSTA ParisTech – UME, 828 Boulevard des Maréchaux, 91762 Palaiseau Cedex, FRANCE
[b] AREVA, 1 Place Jean Millier, 92084 Paris La Défense, FRANCE

Abstract

The aim of this paper is to give a better understanding of damage mechanisms that control lifetime of austenitic stainless steel nuclear components under cyclic loading. The acoustic emission signals were analyzed, in order to identify the acoustic signatures corresponding to a specific damage mode. An unsupervised classification method allows differentiating signals resulting from the plastic deformation or fatigue crack growth. Both phenomena are the two main sources of acoustic emissions in isotropic materials. The main results are the classification of acoustic signals by multivariate statistical methods in different classes. A relation can be established between each class and the present deformation mechanisms and damage, and their order of appearance according to the loading amplitude.

Keywords: Low cycle fatigue; austenitic stainless steel; acoustic emission; multivariate statistical analysis

1-Introduction

Austenitic stainless steels combine good mechanical properties to an excellent corrosion resistance. This combination made this material the most widely used for the construction materials in Nuclear Power Plants (NPPs), especially inside the pressure vessel or in pipes of primary circuits. In such circuits, fluid temperature variations (up to 160°C) between hot and cold branches of mixing tees can induce thermal fluctuations of the fluids large enough to induce thermal fatigue of the pipes [1]. In the primary system, the material is also subjected to a thermo-

_____

* Corresponding author. Tel.: +331-69319735; fax: +331-69319906.
  E-mail address: ammar.ould-amer@ensta-paristech.fr

mechanical cycling caused by temperature gradients during start-ups, shutdowns or operating transients. Consequently, the Low Cycle Fatigue (LCF) is considered as one of the main degradation mechanisms affecting the life of NPPs [2]. Only a thorough knowledge of the phenomena of damage occurring in the material used, on the one hand, and factors influencing its behavior, on the other hand, will simulate and accurately predict the behavior within a structure. It is essential to have phenomenological models representing thermo-mechanical behavior. Understanding the physical mechanisms governing the cyclic behavior and leading to the degradation is a necessary step. Actually, most damage measurements under cyclic loading are based on observation of the surface samples [1-5].

In this study, we focus on another technique for the detection of events during fatigue tests. This technique is Acoustic Emission (AE). Detection and analysis of AE are powerful means for identification of damage phenomena and monitoring of their evolution. AE [6] is a transient wave resulting from the sudden release of stored energy during damage. In the case of austenitic stainless steel materials, various mechanisms act as AE sources including the plastic deformation, martensitic transformation and fatigue crack growth [7]. These three phenomena are the main sources of acoustic emissions in isotropic materials [8]. They generate AE events characterized by specific waveforms. Therefore the population of acoustic even can be heterogeneous, making often difficult to interpret the data in order to correctly identify the damage mechanism of the structure.

A single parameter analysis usually allows differentiating two mechanisms with very different parameters of acoustic signals. This type of analysis as already been applied by Châtellet et al. [9] to study the fatigue behavior of shape memory alloys and Quiong et al. [10] to the fatigue crack pressure pipe material. Also in the case of austenitic stainless steel, Dahmene et al. [11] used waveforms amplitude to monitor crack propagation in a tensile test, considering that signals caused by gliding dislocation and their pinning by solute atoms and crack propagation. However, a conventional analysis based on only one parameter (such as amplitude, energy…) is not sufficient to discriminate the different stages of damage in fatigue tests of stainless steel. So, a statistical method of data analysis is necessary to identify the significant parameters. Pattern recognition techniques can be used [12].

The k-means algorithm [13, 14] is one of the most widely used methods for determining clustering solutions for a particular used-defined number of clusters. This method has already been used by Anastassopoulos and Philippidis [15], Godin et al. [13, 16], on several composites, and by Shaira et al. [7], Ennaceur et al. [17] on 304L stainless steel, and allowed for the identification of different classes of AE signals.

The aim of this study is to investigate the evolution of the damage in the 304L stainless steel under cyclic loading. The damage is measured via the AE technique. The characteristics of different AE sources were studied by conventional methods and multivariate statistical acoustic signals.

2. Material and experiments

2.1. Material

The material used in this study is an AISI type 304L austenitic stainless steel. The chemical composition is given in Table 1.

Table 1. Composition of the AISI 304L stainless steel used in this study (wt %) for the whole matrix and for inclusion.

	Fe	Mn	Si	Ni	Cr	O	Al	Ti
Matrix	Balance	2,24	0,66	10,96	18,65	-	-	-
Inclusion	1.07	23.41	-	-	24.51	38.53	6.18	6.3

The optical microscope observation (Fig.1) reveals the presence of residual ferrite chaplets oriented in the rolling direction and the presence of inclusions randomly distributed in the microstructure, their chemical composition is given in Table 1. The average grain size of this material is about 100 μm in the rolling direction, and 120 μm in the transverse direction.
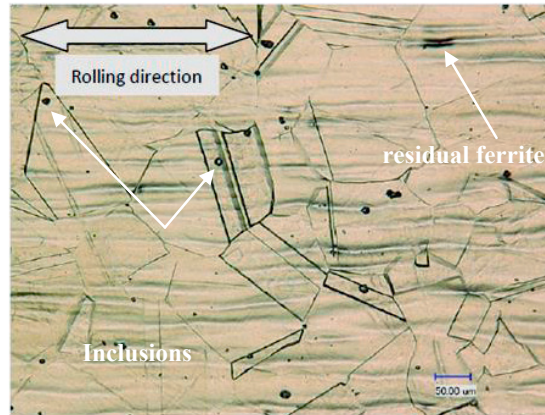

Fig.1. Microstructure of AISI 304L stainless steel observed after chemical etching.

2.2. Test Specimen

The test specimens used are cylindrical with a gauge section of 8 mm in diameter, 22 mm in length and a total length of 135 mm (Fig.2). To minimize the effects of the surface irregularities on the fatigue lives, a final surface preparation is achieved, consisting of a mechanical polishing of the gauge length with silicon carbon paper until grade 4000 and with industrial diamond suspension until grade 9 μm.

2.3. Low Cycle Fatigue (LCF) tests

Low cycle fatigue tests are conducted on a servo-hydraulic machine (MTS 810) (Fig.2) at different total-strain-amplitudes ranging from +/-0.6% to +/-0.2%, in laboratory air and at room temperature.
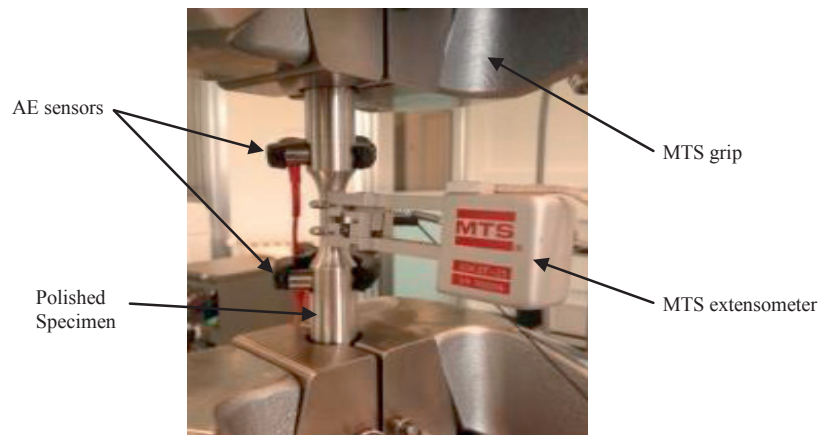

Fig.2. Fatigue sample, with extensometer and AE sensors placed on the machine.

Specimens were generally fatigued until failure unless otherwise specified. The number of cycles to failure is considered as the fatigue life noted N_f. The total-strain-amplitude is controlled by an MTS extensometer, with a root of 10 mm, placed on the gage of the test specimen. The input strain signal was triangular in shape. The basic characterization was based on the results of tests conducted with a constant strain rate of 10^{-3} s^{-1} and a strain ratio $R_\varepsilon = \varepsilon_{min} / \varepsilon_{max} = -1$.

Observations of the fractured surfaces of the specimen and the determination of the chemical composition were carried out in a JEOL Scanning Electron Microscope (SEM).

Observation of the gage of the test specimen during cyclic are performed with a numerical microscope Keyence.

2.3. Acoustic Emission (AE)

Acoustic emission was monitored using a MISTRAS 2001 data acquisition system (Euro Physical Acoustics). Two resonant piezoelectric sensors (Nano 30) were fixed on the surface of the specimen. Silicon grease was used as a coupling agent for sensor/specimen interfaces (Fig.2). A 30 dB recording threshold was determined during the experiments associated to pre-amplifiers of 40 dB and analogical filters with the following bandwidth [200 kHz, 1 MHz]. The acquisition parameters were set as follows: peak definition time 200 µs, hit definition time 400 µs and hit lockout time 1000 µs. AE wave velocity (2100 m/s) was determined before tests using a pencil lead break procedure. Several breaks were performed on the specimen. The average AE wave velocity was then calculated using the difference in arrival time at the two sensors (measured between both signals first peaks). This average AE wave velocity was used for the determination of AE sources location in each test. For each source, the considered signal was the one recorded by the closest sensor in order to reduce effects of attenuation.

AE signal descriptors were calculated in real-time by the data acquisition system. The level of load and of strain as a function of time were also recorded using the same data acquisition system. This setting of the acoustic device is essential, since we must find the right compromise between the risk of recording noise and missing information. To ascertain the acoustic nature of the MTS fatigue machine and the ambient environment, several noise tests were performed with the two transducers mounted on a specimen. The MTS machine was then switched on with both the mean cyclic load and the span setting at zero. This meant that the load was applied just to grip the specimens with no tensile load applied along the length of the specimen. The sources of noise present were the hydraulic pump plus the hydraulic valves and the actuator piston.

The methodology developed to study, explore and analyze the AE data can be decomposed as follows:

1) The first step is obviously data collection. Once the data is available, it is necessary to preprocess which to make the segmentation of acoustic signals as efficiently as possible [18]. The minimum pretreatment is to standardize the data center, to avoid, for example, that some parameters have very large values compared to others.

2) A conventional study of AE signals is performed. It will identify the acoustic signature of certain mechanisms and provide some answers on the chronology of the acoustic activity during fatigue tests.

3) A Principal Component Analysis (PCA) [19] is then performed to find a new basis of eigenvectors by uncorrelated linear combinations of all the selected thereby be reduced to a new orthogonal space descriptors. Then we can reduce the space for example 4 dimensions retaining more than 95% of the information.

4) A statistical analysis of multi-parameter signals AE. It will help to develop a tool to discern the patterns of damage during cycling under different stress amplitudes. At first the "unsupervised" k-means method is used whose aim to identify and classify the major populations of acoustic signatures. Therewith, each acoustic emission signal is characterized by seven parameters (rise time, counts, energy, duration, amplitude, average frequency, counts to peak). Calculating the distance between each vector (signal EA) is carried out using the Euclidean distance in a space of seven dimensions. The EA data processing is done using Matlab software.

The number of signal classes is unknown a priori; a method for validating segmentation Davies and Bouldin [20] was performed, this number is varied between 2 and 10 with 30 iterations to get the best possible result. The best classification is that which minimizes the coefficient of Davies and Bouldin.

3. Results and discussion

3.1. Global behavior

The Cyclic Stress-Strain (CSS) mechanical behavior at different total-strain-amplitudes is represented in Fig.3. Three stages can be observed:
- a slight hardening during the ten first cycles. This phenomenon is awarded to an increase of the dislocation density, in one hand, and of tangles in another hand. Tangles reduce the movement of the gliding dislocation, contributing to the cyclic plasticity [7, 21].
- followed by a weak softening stage. This step is generally coexisted with the introduction of a high density of dislocations or with the formation of structure like walls-channels or labyrinths [5, 21].
- and finally, a stabilization of the stress amplitude stage up to rupture.

This particular behavior has already been observed in same material at room temperature in previous works [1-5].
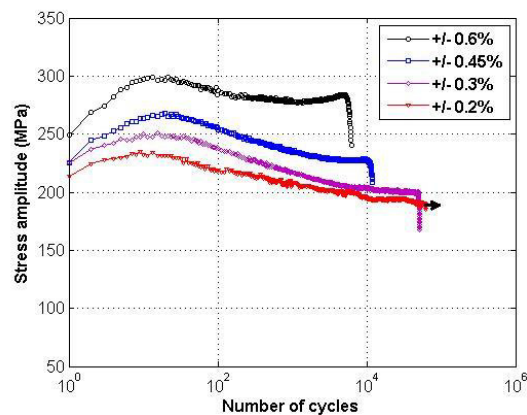

Fig.3. Cyclic evolution of the stress amplitude during strain-controlled fatigue tests.

During hardening/softening stage, cracks appear at the surface of the specimen. However, these cracks have a depth limited to a few microns, and cannot modify the stiffness of the specimen. Microcracks initiated may then propagate and coalesce under the effect of the cyclic loading to form the main crack, which leads to the rupture of the sample [3].

3.2. Analysis of acoustic signals

3.2.1. Conventional analysis

The analysis of AE results of different amplitude of total strain imposed, allows a chronological classification of different stage of damage to be obtained. Fig.4 shows the cumulated AE energy versus the number of cycles. Three areas are observed, that correspond to different stages of the CSS mechanical behavior:

- in the first stage (I), the AE testing system began to receive AE signals from the first cycle, the accumulated energy increases rapidly and stabilizes to about 10 to 20% of the fatigue life. This stage corresponds to the hardening / softening phase of the cyclical behavior of 304L stainless steel.
- in a second stage (II), increased energy accumulated more pronounced compared to the previous stage, it extends up to about 75% of the fatigue life. This stage corresponds to the stabilization of the stress amplitude stage.
- finally, in the last stage (III), the energy accumulated increase rapidly to failure of the specimen. In this stage of fatigue test, the micro-cracks initiated in the previous regime propagate and coalesce to form the main crack.
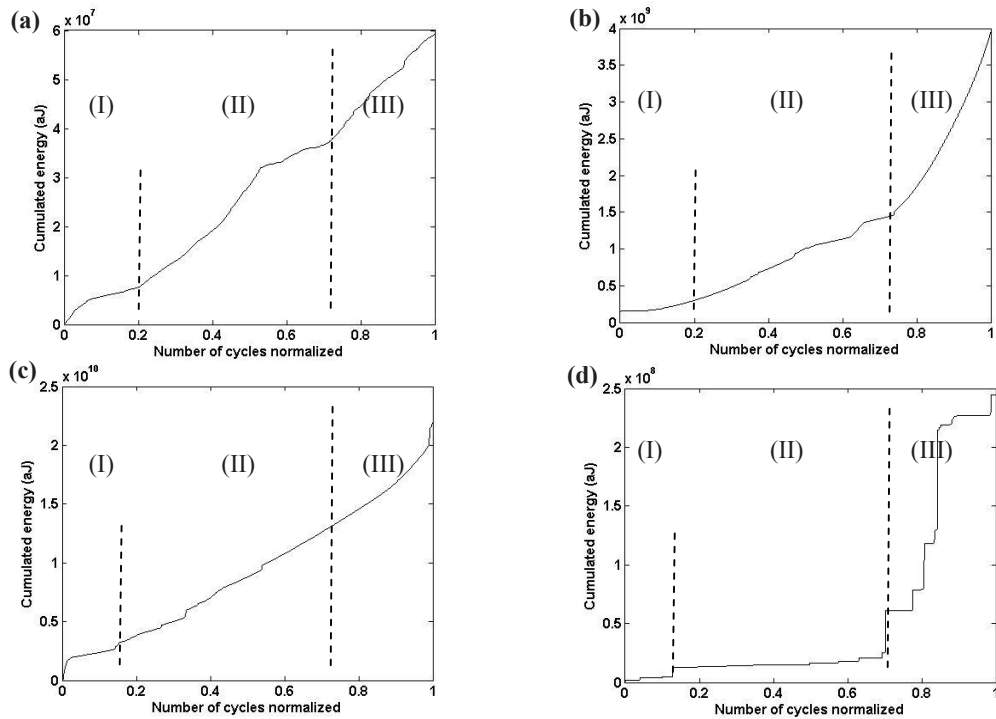

Fig.4. Evolution of the AE cumulative energy during low cycle fatigue tests under different total strain amplitude (a) ±0.2%, (b) ±0.3%, (c) ±0.45% and (d) ±0.6%.

The conventional analysis of the EA during fatigue tests highlights a correlation between the acoustic signals and damage evolution during cycling. But in all fatigue tests, even though the areas identified in relation to the damage corresponding recoveries are uncertain and make assigning a signal to damage that actually occurred, when the AE parameters are in an area recovery. This conclusion is noted by various authors [22-25].

3.2.2. Multivariate statistical analysis

In order to identify the main mechanisms sources activated during the fatigue test, the AE signals are segmented into classes according to the technique of k-means. Several workers participated in some research work on the AE sources during fatigue process [26-32]. According to their results, the main AE sources are plastic deformation of the specimen and crack propagation. Shaira et al. [7] have pointed out that it is possible to classify AE signals by

using the k-means algorithm. They showed that the AE signals may be classified into three clusters that are respectively associated with dislocation movement, crack activity and martensitic transformation.

Using the validation method of Davies and Bouldin (R_{DB}), the segmentation into 4 clusters is one that minimizes the coefficient R_{DB}, for most tests. A fourth population of signals may be due to external noise. Using the K Nearest Neighbors (KNN) method (for more information on this method see [33]) on different classes already separated by the k-means method, with as learning vector signals collected during testing noise signals, 95% of one of the cluster in test amplitude of (± 0.6%) were attributed to external noise, and 100% in tests amplitude of (±0.2%, ±0.3% and ±0.45%). This cluster is later removed from individual files, as this data subset was obviously noise.

Fig.5 shows the distribution of duration versus counts of signals received during LCF tests under ±0.3% total strain amplitude, segmented by k-means method. The three clusters are always present and have the same mean characteristic independently of the strain amplitude. The segmentation of the AE data is very reproducible.
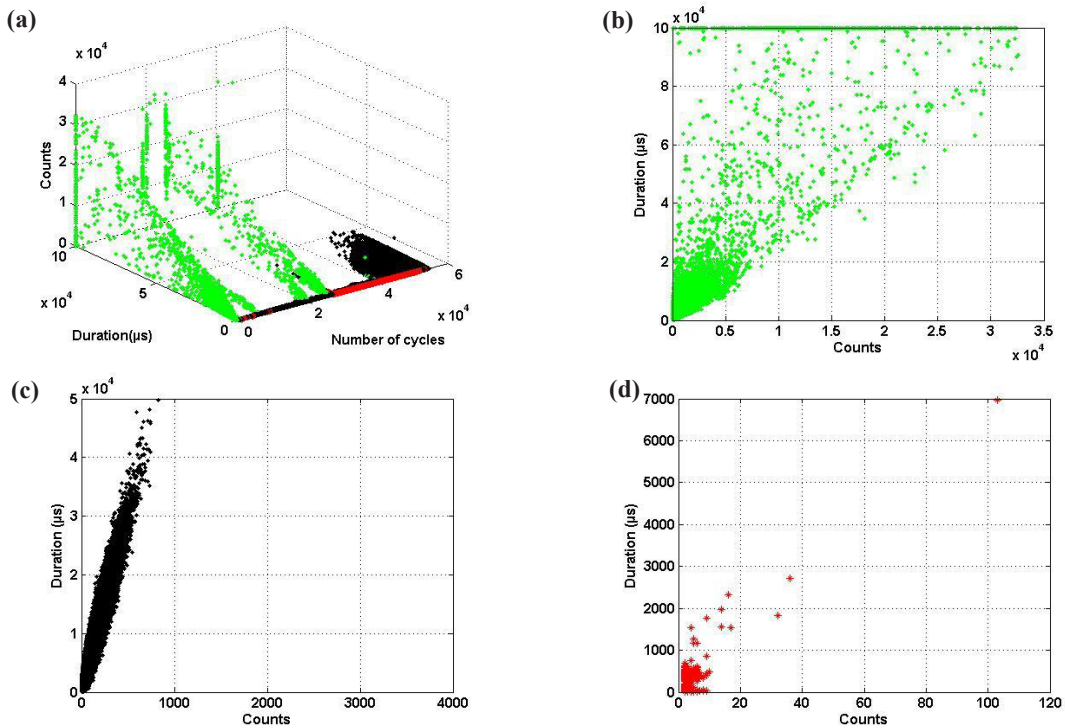

Fig.5. Clustering results during low cycle fatigue test under ±0.3% total strain amplitude: (a) original data: counts and duration distribution with number of cycles, and duration versus counts of different clusters (b) cluster 1, (c) cluster 2, and (d) cluster 3.

From the AE distributions obtained after pattern recognition, some important differences in the AE signals characteristics are found. Indeed, three types of signals are identified to be distinct. Table 2 summarizes the mean characteristic of the threes clusters and their schematic representation of waveform.

The AE in cluster 1 is characterized by a wide range of counts and duration, causing a continuous signal; they are the largest among the three clusters. The cluster 2 signals have a shorter duration and counts. The last cluster (cluster 3) corresponds to almost impulse signals, it is constituted by very short signals mainly in the last of the tests.

Table2. AE parameters for the threes clusters and a schematic representation of the waveform.
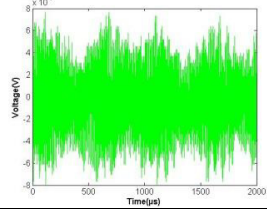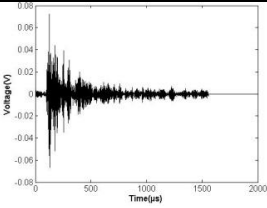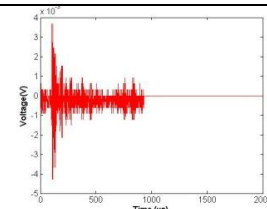
Clusters	Means parameters		Schematic representation of the waveform
1	Duration (μs) Counts Rise time (μs) Amplitude (dB) Energy (aJ)	2561 581 2256 38 5420	
2	Duration (μs) Counts Rise time (μs) Amplitude (dB) Energy (aJ)	328 50 11 57 7911	
3	Duration (μs) Counts Rise time (μs) Amplitude (dB) Energy (aJ)	15 3 1 33 28.502	

Fig.6 shows cumulative curves of the three clusters in terms of the AE hits' energy. The energy of AE signals in cluster 1 increase stably at the beginning of the test. The AE activities are very energetic in the regime of hardening / softening of the mechanical behavior described above. This is consistent with the emission being generated by collective dislocation motion. In stabilization of stress in the mechanical behavior, dislocations arrange in more complex structures or in persistent slip bands [21], the distance traveled by the dislocations in this stage is so small and can not be detected by EA. The AE signals detected at this stage are only generated by the plastic zone formation in ahead of the crack tip [34].
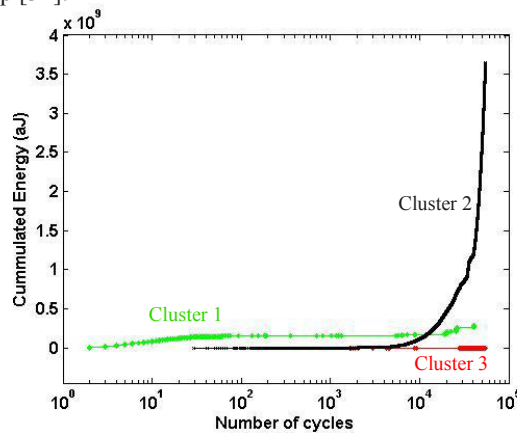

Fig.6. Evolution of the AE cumulative energy during low cycle fatigue test ±0.3% total strain amplitude for Clustering results.

The energy of AE signals in cluster 2 increase slowly before 4000 cycles, but rapidly after 4000 cycles, which was consistent with the trend of cracks from initiation to propagation during the fatigue test.

Acoustic activity of cluster 3 is the smallest. Signals of this class appear at end of test. Muller et Al. [35], observed in austenitic stainless steel a second hardening at the end of the test. This author associated with a progressive plastic strain induced martensitic phase transformation is a possible origin of the secondary hardening. Vincent et al [1] showed that the levels of secondary hardening and the volumic fraction of the magnetic phase are clearly linked at room temperature. The late appearance of cluster 3, suggesting that the signals of this class are associated with the phase transformation.

4. Conclusions

The low cycle fatigue of 304L stainless steel was monitored by AE for different total strain amplitudes. The evolution of the activity of the EA during fatigue tests highlights a correlation between the acoustic signals and damage evolution. But in all fatigue tests, even though the areas identified in relation to the damage corresponding are uncertain and make assigning a signal to damage that actually occurred, when the AE parameters are in an area recovery.

Based on k-means cluster algorithm, different AE sources are classified. And the results indicate that the AE characteristics of different AE sources, such as plastic deformation, cracking and martensitic transformation, differ significantly, which could be of much help in analyzing and judging the fatigue situation.

References

[1] L. Vincent, J-C. Le Roux, S. Taheri, On the high cycle fatigue behavior of a type 304L stainless steel at room temperature, International Journal of Fatigue 38 (2012) 84-91.

[2] L.De Baglion, J. Mendez, Low cycle fatigue behavior of a type 304l austenitic stainless steel in air or in vacuum, at 20 °C or at 300 °C: relative effect of strain rate and environment, Procedia Engineering 2 (2010) 2171-2179.

[3] P. Mu, V. Aubin, I. Alvarez-Armas, A. Armas, Influence of the crystalline orientations on microcrack initiation in low-cycle fatigue, Materials Science and Engineering: A. 573 (2013) 45-53.

[4] N. Haddar, A. Köster, Y. Kchaou, L. Remy, Thermal–mechanical and isothermal fatigue of 304L stainless steel under middle range temperatures, Comptes Rendus Mécanique, 340, Issue 6 (2012) 444-452.

[5] A. Le Pécheur,F. Curtit, M. Clavel, J. Stephan, C. Rey, P. Bompard, Polycrystal modelling of fatigue: pre-hardening and surface roughness effects on damage initiation for 304l stainless steel, International Journal of Fatigue 45 (2012) 48-60.

[6] A.G. Beattie, Acoustic emission, principles and instrumentation. J Acoust Emission 2 (1983) 95–128.

[7] M. Shaira, N. Godin, P. Guy, L. Vanel, J. Courbon, Evaluation of the strain-induced martensitic transformation by acoustic emission monitoring in 304L austenitic stainless steel: Identification of the AE signature of the martensitic transformation and power-law statistics, Materials Science and Engineering: A. 492, Issues 1–2 (2008) 392-399.

[8] L. Calabrese, G. Campanella, E. Proverbio, Identification of corrosion mechanisms by univariate and multivariate statistical analysis during long term acoustic emission monitoring on a pre-stressed concrete beam, Corrosion Science 73 (2013) 161-171.

[9] C. Dunand-Châtellet, Z. Moumni, Experimental analysis of the fatigue of shape memory alloys through power-law statistics, International Journal of Fatigue, 36, Issue 1 (2012) 163-170.

[10] Qiong Ai, Cai-Xue Liu, Xiang-Rong Chen, Pan He, Yao Wang, Acoustic emission of fatigue crack in pressure pipe under cyclic pressure, Nuclear Engineering and Design, 240, Issue 10 (2010) 3616-3620.

[11] F. Dahmene, A. Laksimi, S. Hariri, C. Hervé, L. Jaubert, M. Cherfaoui, A. Mouftiez, Acoustic wave propagation in austenitic stainless steel AISI 304L: Application examples, International Journal of Pressure Vessels and Piping, 92 (2012) 77-83.

[12] A.A. Anastassopoulos, Signal processing and pattern recognition of AE signatures, in: Experimental Analysis of Nano and Engineering Materials and Structures, Springer Netherlands, Dordrecht, The Netherland, (2007) 929.

[13] N. Godin, S. Huguet, R. Gaertner, Integration of the Kohonen's self-organising map and k-means algorithm for the segmentation of the AE data collected during tensile tests on cross-ply composites, NDT & E International, 38, Issue 4 (2005) 299-309.

[14] Aristidis Likas, Nikos Vlassis, JakobJ. Verbeek, The global k-means clustering algorithm. Pattern Recognition 36 (2003) 451 – 461.

[15] A.A. Anastassopoulos, T.P. Philippidis, Clustering methodology for the evaluation of acoustic emission from composites, J. Acoust Emission, 13 (1995) 1–22.

[16] N. Godin, S. Huguet, R. Gaertner, Clustering of acoustic emission signals collected during tensile tests on unidirectional glass/polyester composite using supervised and unsupervised classifiers. NDT & E Int, 37(2004) 253–64.

[17] C. Ennaceur, A. Laksimi, C. Hervé, M. Cherfaoui, Monitoring crack growth in pressure vessel steels by the acoustic emission technique and the method of potential difference, International Journal of Pressure Vessels and Piping, 83, Issue 3 (2006) 197-204.

[18] G. Dreyfus, J.M. Martinez, M. Samuelides, M. B. Gordon, F. Badran, S. Thiria, L. Hérault, Apprentissage statistique, Eyrolles, 2008.

[19] C. Ding, X. He, K-means clustering via principal component analysis, Proc. of int'l conf. machine learning, (2004) 225-232.

[20] D.L. Davies, D.W. Bouldin, A cluster separation measure, IEEE Trans Pattern Anal Machine Intell, 1 (1979) 224–227.

[21] M. Gerland, R. Alain, B. Ait Saadi, J. Mendez, Low cycle fatigue behaviour in vacuum of a 316l-type austenitic stainless steel between 20 and 600°c - part ii: dislocation structure evolution and correlation with cyclic behaviour, Materials Science and Engineering: A, 229 (1997) 68-86.

[22] W. Eckles, J. Awerbuch, Monitoring Acoustic Emission in cross-ply graphite/epoxy laminates during fatigue loading. Journal of Reinforced Plastics Composites, 7 (1988) 265-283.

[23] J. Awerbuch, S. Ghaffari, Tracking progression of matrix splitting during static loading through Acoustic Emission in notched unidirectional graphite/epoxy composites, in: ASNT Proc. of the 6th International Symposium on Acoustic Emission from Composite Materials, (1986) 575-585.

[24] C. G. Gustafson, R. B. Selden, Monitoring fatigue damage in CFRP using Acoustic Emission and radiographic techniques in Delamination and debonding of materials, in: W. S. Johnson Ed. ASTM STP 876, (1985) 448-464.

[25] J. Block, Monitoring of defect progression by Acoustic Emission in Characterization, analysis and significance of defects in Composite materials, AGARD CP N°.355 (1983) 1-11.

[26] K. Máthis, D. Prchal, R. Novotny´ , P. Hähner, Acoustic emission monitoring of slow strain rate tensile tests of 304L stainless steel in supercritical water environment, Corros. Sci. 53 (2011) 59–63.

[27] G. Du, W.K. Wang, S.Z. Song, S.J. Jin, Detection of corrosion on 304 stainless steel by acoustic emission measurement, Anti-Corros. Method M 57 (2010) 126–132.

[28] J. Kovacˇ, C. Alaux, J. Marrow, E. Govekar, A. Legat, Correlations of electrochemical noise, acoustic emission and complementary monitoring techniques during intergranular stress-corrosion cracking of austenitic stainless steel, Corros. Sci. 52 (2010) 2015–2025.

[29] K.Y. Sung, I.S. Kim, Y.K. Yoon, Characteristics of acoustic emission during stress corrosion cracking of inconel 600 alloy, Scripta Mater. 37 (1997) 1255–1262.

[30] M.G. Alvarez, P. Lapitz, J. Ruzzante, AE response of type 304 stainless steel during stress corrosion crack propagation, Corros. Sci. 50 (2008) 3382–3388.

[31] J. Kovacˇ, M. Leban, A. Legat, Detection of SCC on prestressing steel wire by the simultaneous use of electrochemical noise and acoustic emission measurements, Electrochim. Acta 52 (2007) 7607–7616.

[32] H. Shaikh, R. Amirthalingam, T. Anita, N. Sivaibharasi, T. Jaykumar, P. Manohar, H.S. Khatak, Evaluation of stress corrosion cracking phenomenon in an AISI type 316LN stainless steel using acoustic emission technique, Corros. Sci. 40 (2007) 740–765.

[33] K. Hattori, M. Takahashi, A new nearest-neighbor rule in the pattern classification problem. Pattern Recogn., 32 (1999) 425–32.

[34] Wen-Fung Wang, Meng-Jung Wu, Effect of silicon content and aging time on density, hardness, toughness and corrosion resistance of sintered 303LSC–Si stainless steels, Materials Science and Engineering: A 425, Issues 1–2 (2006) 167-171.

[35] C. Muller-Bollenhagen, M. Zimmermann, H.J. Christ, Very high cycle fatigue behaviour of austenitic stainless steel and the effect of strain-induced martensite, Int J Fatigue, 32 (2010) 936–42.